# High-Impact Hydrologic Events and Atmospheric Rivers in California: An Investigation using the NCEI Storm Events Database

**Allison M. Young[1], Klint T Skelly[2], and Dr. Jason M. Cordeira[1]**

[1]Plymouth State University

[2]NOAA/National Weather Service, Pueblo, CO

Corresponding author: Dr. Jason M. Cordeira (j_cordeira@plymouth.edu)

Allison M. Young (amy1000@plymouth.edu)

Klint T Skelly (klint.skelly@noaa.gov)

**Key Points:**

- High-impact hydrologic events (e.g., floods, flash floods, and debris flows) occur in conjunction with atmospheric rivers in California
- A majority of floods and debris flows occur in association with landfalling atmospheric rivers in the cold-season over northern California
- A majority of flash floods occur in association with a flow pattern that resembles the warm-season North American Monsoon in southern California



This article has been accepted for publication and undergone full peer review but has not been through the copyediting, typesetting, pagination and proofreading process which may lead to differences between this version and the Version of Record. Please cite this article as doi: 10.1002/2017GL073077

**Abstract**

Atmospheric rivers (ARs) are long, narrow corridors of enhanced integrated water vapor and integrated vapor transport that can result in high-impact hydrologic events (HIHEs) including floods, flash floods, and debris flows. This study examined the relationship between HIHEs and ARs in California for 10 water years using the National Centers for Environmental Information Storm Events Database and a catalog of landfalling ARs provided by Rutz et al. [2013]. Results illustrated that HIHEs related to floods and debris flows are commonly associated with ARs during the cold-season across northern California, whereas HIHEs related to flash floods are commonly not associated with ARs during the warm-season across southern California. Composite analyses illustrated that HIHEs associated with landfalling ARs are associated with synoptic-scale flow patterns that support southwesterly water vapor flux that aligns favorably with California coastal topography to maximize upslope flow and orographic precipitation.

## 1 Introduction

Floods, flash floods, and debris flows (e.g., shallow, rain-induced landslides) can be hazards associated with heavy precipitation. Floods are defined as the overflowing of water from normal confines or the accumulation of water in areas where water usually does not occur [*AMS,* 2016a], and flash floods are defined as floods that occur more rapidly, with little to no warning [*AMS,* 2016b]. Debris flows are commonly defined as hybrids of landslides and floods that result in a flowing mixture of equal parts sediment and water [*NOAA–USGS Debris Flow Task Force,* 2005]. Floods and flash floods are responsible for 75% of all presidential disaster declarations in the U.S. [*NOAA,* 2016], whereas landslides, including debris flows, are responsible for 25–50 deaths and damages >$2 billion annually in the U.S. [*NOAA–USGS Debris Flow Task Force,* 2005]. The purpose of this study is to investigate the synoptic-scale meteorological conditions associated with floods, flash floods, and debris flows [e.g., high-impact hydrological events (HIHEs)] in California.

## 2 Background

Heavy precipitation events (e.g., 72-h precipitation accumulation >300–400 mm) over the U.S. are frequently caused by warm-season severe convective systems and tropical cyclones over the southern Plains and Southeast, and by landfalling winter storms along the West Coast [*Ralph and Dettinger,* 2012]. The latter occur predominantly in conjunction with orographic precipitation in the warm sector of these winter storms along a corridor of enhanced atmospheric water vapor known as an atmospheric river (AR) [*Ralph et al.,* 2004]. ARs are long, narrow corridors of enhanced integrated water vapor (IWV) and integrated vapor transport (IVT) that account for ~90% of all poleward moisture transported globally on only 10% of the global surface [*Zhu and Newell,* 1998; *Ralph et al.,* 2004; *Neiman et al.,* 2008a,b; among others]. ARs typically contain IVT magnitudes ≥250 kg $m^{-1}$ $s^{-1}$ and IWV values ≥20 mm [*Ralph et al.,* 2011] in a region >2,000 km long and <1,000 km wide [*Zhu and Newell,* 1998] that is found in the warm sector of extratropical cyclones, ahead of cold fronts, and along low-level jet streams [*Zhu and Newell,* 1998; *Ralph et al.,* 2004; *Bao et al.,* 2006; *Stohl et al.,* 2008; *Cordeira et al.,* 2013]. Water vapor flux along ARs commonly

influences heavy precipitation over California during the cold season from October to March as their parent winter storms follow a more southerly storm track [*Neiman et al.,* 2008b].

ARs that make landfall in California typically contain 75% of their water vapor transport in the lowest 2.25 km of the atmosphere [*Ralph et al.,* 2005] and last for ~20–30 hours [*Ralph et al.,* 2013]. The low-level transport of moisture along ARs from over the Northeast Pacific toward the U.S. West Coast can result in intense orographic precipitation in the Coast Ranges, Transverse Ranges, and Sierra Nevada [*Lin et al.,* 2001; *Ralph et al.,* 2006; *Smith et al.,* 2010; among others]. Case studies of individual events have identified that the intensity and duration of orographic precipitation associated with landfalling ARs in regions of complex terrain can often result in HIHEs, especially over the western U.S. [*Wieczorek and Glade,* 2005; *Restrepo et al.,* 2008; *Rutz et al.,* 2013; among others]. The twin objectives of this study are to identify what fraction of California HIHEs are associated with landfalling ARs and to illustrate the synoptic-scale meteorological conditions associated with AR-related HIHEs.

## 3 Data and methodology

This study focuses on reports of floods, flash floods, and debris flows obtained from the National Centers for Environmental Information (NCEI) Storm Events Database [*NCEI Storm Events Database, 2016*] for 10 National Weather Service (NWS) County Warning Areas (CWAs) over northern and southern California during a 10-water year (WY) period between 1 October 2004 and 30 September 2014. The five northern CWAs are overseen by the Monterey (MTR), Sacramento (STO), Eureka (EKA), Reno (REV), and Medford (MFR) weather forecast offices (WFOs), whereas the five southern CWAs are overseen by the Phoenix (PSR), San Diego (SGX), Los Angeles (LOX), Las Vegas (VEF), and Hanford (HNX) WFOs. The reports are investigated over the full WY, the cool-season portion of the WY during October–March, and the warm-season portion of the WY during April–September. The NCEI Storm Events Database is used in this study because of its official use in the NOAA community and because it has not yet been used extensively to study the impacts of landfalling ARs. Presentation of spatial statistics of HIHE reports allows double counting across CWAs (e.g., a report on the same day in two different CWAs), whereas presentation of temporal statistics and composite analyses use unique days with HIHE reports across CWAs (e.g., a HIHE day for northern CA).

The HIHE days are compared to days with landfalling ARs using an "AR catalog" produced by Rutz et al. [2013]. The AR catalog identifies ARs as locations with IVT magnitudes ≥250 kg $m^{-1}$ $s^{-1}$ that are ≥2,000 km in length every six hours from 1948–2015 using the National Centers for Environmental Prediction (NCEP)–National Center for Atmospheric Research (NCAR) Reanalysis dataset on a global 2.5° latitude × 2.5° longitude resolution grid [*Kalnay et al.,* 1996]. The grid points from the AR catalog used in this study are 40.0°N, 235.0°E; 42.5°N, 235.0°E; 37.5°N, 237.5°E; 35.0°N, 240.0°E; and 32.5°N, 242.5°E along the California coast. A HIHE day is associated with an AR if an AR is located along the California coast on the day of or the day before the HIHE report. This categorization attempted to correct for a temporal lag among the AR, precipitation, runoff, and the HIHE report.

The common synoptic-scale flow patterns on HIHE days associated with ARs are presented as composite analyses constructed from a combination of reanalysis and operational data from the NCEP–Climate Forecast System Reanalysis (CFSRv2) dataset [*Saha et al.*, 2010; *Saha et al.*, 2014]. The CFSRv2 data is contained on a grid that spans vertically from 1000-hPa to 1-hPa on 37 isobaric levels, horizontally with a resolution of t384 (~38 km) that is obtained on a 0.5° latitude by 0.5° longitude grid, and temporally every six hours. All composite analyses are constructed from 1200 UTC data on the day of the HIHE report. All variables shown in composite analyses are provided by NCEP except for the vector quantity IVT, which is calculated according to the methodology of Neiman et al. [2008b] as:

$$\overrightarrow{IVT} = \frac{1}{g}\int_{1000\ hPa}^{300\ hPa} q\vec{V}\,dp \qquad \text{(Eq. 1)}$$

where $g$ is the gravitational acceleration, $q$ is specific humidity, and $V$ is total horizontal vector wind.

The NCEP Stage-IV 24-h quantitative precipitation estimates (QPE) dataset is used to investigate CWA areal-averaged precipitation on HIHE days associated with ARs and not associated with ARs. The QPE dataset produced by regional River Forecast Centers in the continental United States is constructed from combinations of regional radar and gauge precipitation estimates, known as multisensory precipitation analyses. The regional datasets combine to create a national mosaic of 24-h QPE on a 4-km grid [*NCEP/EMC,* 2016]. This study (1) averages the QPE over each California CWA for the 48-h period on the day of and day before a HIHE report in order to identify whether or not mean areal QPE on HIHE days associated with ARs differs from mean areal QPE on HIHE days not associated with ARs, and (2) compares these QPE values to the 10-WY climatology of mean areal QPE on days with >0 mm of precipitation. The former is compared to the latter as its "rank" in the climatology (i.e., a QPE in the 95$^{th}$ percentile is higher than 95% of the days with >0 mm). These statistics were only calculated for CWAs that contained more than one HIHE report.

## 4 Results

### 4.1 HIHE distributions

A total of 1,415 HIHE reports in California during the 10-year period of study reduced to 580 HIHE days across the different CWAs (Fig. 1a); many days contained more than one report. A large majority (82.9%) of HIHE days occurred over southern California; however, a larger fraction of HIHEs were associated with landfalling ARs across northern California (80.8%) as compared to southern California (41.8%). The 580 HIHE days across the different CWAs, when combined, reduced to 364 unique HIHE days for the state of California (Fig. 1b). A larger number of HIHE days statewide occurred during the warm-season (57.1%) as compared to the cold-season (42.9%). Conversely, a larger fraction of HIHE days associated with ARs occurred in the cold-season (78.2%) as compared to the warm-season (25.0%), which corresponded to similar values obtained by Neiman et al. [2008b] and Ralph and Dettinger [2012]. The 580 HIHE days across different CWAs, when combined by region, reduced to 88 unique HIHE days for northern California and 301 unique HIHE days for southern California (Figs. 1c,d). Note the sum is higher than 364 because some HIHE days contained reports in both northern California and southern California. A

larger number of HIHE days across northern California occurred during the cold-season (62.5%) as compared to the warm-season (37.5%), whereas a larger number of HIHE days across southern California occurred during the warm-season (60.8%) as compared to the cold-season (39.2%). The fraction of these HIHE days that are associated with ARs was higher over northern California (63.6%) as compared to southern California (39.2%).

The 1,415 HIHE reports over California were comprised of 395 flood reports, 895 flash flood reports, and 125 debris flow reports that occurred on 126 unique flood days, 260 unique flash flood days, and 84 unique debris flow days (Fig. 2). A large majority of HIHE days that were associated with flash floods (Fig. 2a) were not associated with ARs and occurred during the warm-season (Fig. 2b) over southern California (e.g., see Fig. 2 and related text from Ralph et al. [2014]). Flood and debris flow days comprised a large majority of HIHE days during the cold-season at all locations, with the highest fraction of each associated with ARs over northern California.

4.2 HIHE composite analyses

Composite analysis of sea-level pressure (SLP), IWV, and IVT on flood, flash flood, and debris flow days across California associated with ARs (Figs. 3a,c,e) and not associated with ARs (Figs. 3b,d,f) illustrated respectively similar synoptic-scale patterns over the Northeast Pacific. The HIHE days associated with ARs featured a 1004-to-1008-hPa low pressure system over the Gulf of Alaska and a ~1016-to-1020-hPa high pressure system over a broad region of the subtropical Northeast Pacific that resulted in a general westerly geostrophic flow toward the California coast. This westerly flow contained corridors of weak IWV values of ~20 mm and west-southwest IVT magnitudes of ~250 kg $m^{-1}$ $s^{-1}$. Alternatively, the HIHE days not associated with ARs featured a weak region of ~1012-hPa low pressure located over the Alaskan Panhandle, a broad ~1020-hPa anticyclone located over the midlatitude Northeast Pacific, and a weak inverted trough located over central California and western North America containing enhanced IWV >30 mm. This synoptic-scale pattern mimics a warm-season flow pattern across southern California and closely resembled the type-IV monsoon synoptic pattern as defined by Maddox et al. [1980].

Composite analyses of SLP, IWV, and IVT as in Fig. 3 partitioned for HIHE days associated with ARs across northern California and southern California (Fig. 4) removed composite smear in conjunction with averaging landfalling ARs at many different locations along the >1,300 km California coastline. These composite analyses illustrated that HIHE days associated with landfalling ARs were generally related to more characteristic IWV values >22.5–25.0 mm and IVT magnitudes that approach 500 kg $m^{-1}$ $s^{-1}$. On average, the HIHE days associated with ARs across northern California occurred in conjunction with IVT magnitudes that were 150–200 kg $m^{-1}$ $s^{-1}$ higher and IWV values that are ~2.5–5.0 mm lower than those across southern California. This dichotomy suggests that landfalling ARs that produce HIHEs across northern California generally contain stronger wind speeds, which can be inferred from the magnitude of the composite SLP gradient, whereas landfalling ARs that produce HIHEs across southern California generally contain higher amounts of water vapor. The composite analyses also illustrated that HIHE days associated with ARs across northern and southern California occurred in conjunction with west-southwest oriented IVT (i.e., ARs). This AR orientation compares favorably with the orientations of the California Coast Ranges and the Transverse Mountain Ranges (not shown), respectively, which can influence the intensity of orographic precipitation [*Ralph et al.*, 2006].

4.3 Precipitation analyses

The CWA 48-h mean areal QPE rank for HIHE days associated with ARs and not associated with ARs is presented in Fig. 5. HIHE days associated with ARs generally contained a higher QPE rank than HIHE days not associated with ARs with a few exceptions (e.g., flood days at PSR and flash flood days at REV and PSR). The HIHE days associated with ARs generally contained QPE values that ranked in the top 5% (>95$^{th}$ percentile) of all 48-h periods with >0 mm precipitation during the 10-WY study, whereas the HIHE days not associated with ARs generally contained QPE values that ranked in the middle 50% of the QPE distribution.

## 5 Concluding discussion

A majority of extreme precipitation events in California are associated with landfalling ARs that may produce floods, flash floods, and debris flows [i.e., high-impact hydrological events (HIHEs)]. This study identified a 10-WY climatology of HIHEs over California from the NCEI Storm Events Database and subsequently illustrated the synoptic-scale flow patterns on HIHE days associated with ARs. The 10-WY period contained 1,415 HIHE reports over California that occurred on 364 unique days. A large majority of these HIHE days occurred during the warm-season over southern California in conjunction with flash floods, whereas a large majority of HIHE days associated with ARs occurred during the cold-season over northern California in association with floods and debris flows.

Composite analyses of SLP, IWV, and IVT on HIHE days illustrated that HIHEs occurred in association with a region of lower SLP of varying strength located over the Gulf of Alaska and a region of higher SLP of varying strength located over the Central North Pacific that resulted in westerly geostrophic flow. This westerly flow contained enhanced IWV values >20 mm and IVT magnitudes >250 kg m$^{-1}$ s$^{-1}$. When the composite analyses for HIHE days associated with ARs were bifurcated into locations across northern California and southern California, IWV values and IVT magnitudes increased to >22.5–25 mm and >500 kg m$^{-1}$ s$^{-1}$, respectively, along a corridor that palpably resembled a landfalling AR. The unique composite analysis illustrated that flash flood days across southern California tended to occur on days with synoptic-scale flow patterns that resembled the warm-season North American monsoon. The composite analyses for HIHE days associated with ARs also highlighted that landfalling ARs across northern and southern California contained west-southwest oriented IVT. This IVT direction was generally perpendicular to the Coastal Ranges and Transverse Ranges, which can maximize upslope water vapor flux and orographic precipitation.

An analysis of 48-h mean areal QPE illustrated that HIHE days associated with ARs occurred in conjunction with QPE in the top 5% of its distribution, whereas those not associated with ARs occurred in conjunction with QPE in the middle 50% of its distribution with few exceptions. Although this analysis does not necessarily identify the characteristics that define whether or not an AR will produce extreme precipitation or a HIHE, it does provide insight into the likely processes associated with ARs that lead to extreme precipitation and HIHEs. For example, for constant geomorphic conditions (e.g., slope, land cover, soil moisture), a HIHE may be more likely associated with a landfalling AR owing to stationary precipitation forced by topography and relatively long duration that produces top-

5% 48-h mean areal QPE amounts that can saturate soils and lead to enhanced run off and streamflow. Alternatively, a HIHE that is not associated with an AR under similar conditions may be more likely in conjunction with more localized higher precipitation intensity and shorter durations that produce much lower 48-h mean areal QPE amounts. These results motivate future work that could investigate localized 1-, 3-, and 6-h precipitation rates [*Stock and Bellugi*, 2011; *Collins et al.*, 2012; among others], and their mesoscale and synoptic-scale precipitation processes that can better illustrate this spectrum of precipitation rate and durations that leads to HIHEs.

This study illustrated that HIHE days contained within the NCEI Storm Events Database for CWAs across California can be attributed to landfalling ARs and their associated precipitation extremes. This attribution is largely valid for HIHE days across northern California in the cold season and not necessarily valid for HIHE days across southern California during the warm season. Approximately 57% of all HIHE days in California occurred during the warm-season, mostly in conjunction with flash floods, and 75% of these HIHE days were not associated with ARs. The composite analysis of flash flood days across California illustrated the climatological warm-season flow pattern for precipitation across southern California and closely resembled the type-IV monsoon synoptic pattern as defined by Maddox et al. [1980]. This result motivates additional future work that could focus on the role of the North American monsoon and other non-AR processes that produce HIHEs across California.



**Acknowledgments, Samples, and Data**

Support for this project was provided by the State of California-Department of Water Resources award #4600010378 and the U.S. Army Corps of Engineers award #W912HZ-15-2-0019, both as part of broader projects led by the University of California San Diego, Scripps Institution of Oceanography's Center for Western Weather and Water Extremes. Data used in this study are cited in the references and can be accessed through the methodologies mentioned in the third section of this paper. For any questions, please feel free to contact any of the authors. The authors would like to thank Nina Oakley (Desert Research Institute), Dr. David Lavers (European Centre for Medium-Range Weather Forecasts), Dr. Amy Villamagna (Plymouth State University), and Dr. Eric Hoffman (Plymouth State University) who each provided valuable guidance during the completion of two M.S. theses that contained a portion of the results presented in this manuscript.

**References**

AMS (2016a), *Flood – AMS Glossary*. Available from: glossary.ametsoc.org/wiki/Flood (Accessed 21 April 2016)

AMS (2016b). *Flash Flood – AMS Glossary.* Available from: glossary.ametsoc.org/wiki/Flood (Accessed 21 April 2016)

Bao, J.-W., S. A. Michelson, P.J. Neiman, F. M. Ralph, and J. M. Wilczak (2006), Interpretation of enhanced integrated water vapor bands associated with extratropical cyclones: their formation and connection to tropical moisture. *Mon. Wea. Rev.*, 134, 1063–1080, doi:10.1175/MWR3123.1.

Collins, B. D., J. D. Stock, K. A. Foster, M. P. W. Whitman, and N. E. Knepprath (2012), Monitoring the subsurface hydrologic response for precipitation-induced shallow landsliding in the San Francisco Bay area, California, USA. At Landslides and Engineered Slopes: Protecting Society through Improved Understanding. Proc. XI International Symposium on Landslides, Banff, Alta., 2–8 June 2012. 2, 1249–1255.

Cordeira, J. M., F. M. Ralph, and B. J. Moore (2013), The development and evolution of two atmospheric rivers in proximity to western North Pacific tropical cyclones in October 2010. *Mon. Wea. Rev.*, 141, 4234–4255, doi:10.1175/MWR-D-13-00019.1.

Kalnay, E., and Coauthors (1996), The NCEP/NCAR 40-year reanalysis project. *Bull. Amer. Meteor. Soc.*, 77, 437–471, doi:10.1175/1520-0477(1996)077<0437:TNYRP>2.0.CO;2.

Lin, Y. L., T. A. Wang, M. L. Kaplan, and R. P. Weglarz (2001), Some common ingredients for heavy orographic rainfall. *Wea. Forecasting,* 16, 633–660, doi:10.1175/1520-0434(2001)016<0633:SCIFHO>2.0.CO;2.

Maddox, R. A., F. Canova, and L. R. Hoxit (1980), Meteorological characteristics of flash flood events over the western United States. *Mon. Wea. Rev.*, 108, 1866–1877, doi:10.1175/1520-0493(1980)108<1866:MCOFFE>2.0.CO;2.

NCEI Storm Events Database (2016), *Search Results for all U.S. States and Areas, Event Types: Debris Flow.* Available from : https://www.ncdc.noaa.gov/stormevents/listevents.jsp?eventType=%28Z%29+Debris+Flow&beginDate_mm=10&beginDate_dd=01&beginDate_yyyy=2004&endDate_mm=09&endDate_dd=30&endDate_yyyy=2014&hailfilter=0.00&tornfilter=0&windfilter=000&sort=DT&submitbutton=Search&statefips=-999%2CALL (Accessed 16 November 2016)

NCEP/EMC (2016), *National Stage IV QPE Product.* Available from: http://www.emc.ncep.noaa.gov/mmb/ylin/pcpanl/stage4/ (Accessed 21 October 2016)

Neiman, P.J., F.M. Ralph, G.A. Wick, Y. Kuo, T.Wee, Z. Ma, G.H. Taylor, and M.D. Dettinger (2008a), Diagnosis of an intense atmospheric river impacting the Pacific Northwest: storm summary and offshore vertical structure observed with COSMIC satellite retrievals. *Mon. Wea. Rev.*, 136, 4398–4420, doi:10.1175/2008MWR2550.1.

Neiman, P. J., F. M. Ralph, G. A. Wick, J. D. Lundquist, and M. D. Dettinger (2008b), Meteorological characteristics and overland precipitation impacts of atmospheric rivers affecting the West Coast of North America based on eight years of SSM/I satellite observations. *J. Hydrometeor.*, 9, 22–47, doi:10.1175/2007JHM855.1.

NOAA (2016), *Flood related hazards.* Available from: http://www.floodsafety.noaa.gov/hazards.shtml (Accessed 8 November 2016)

NOAA-USGS Debris Flow Task Force (2005), NOAA-USGS debris-flow warning system—Final report: *U.S. Geological Survey Circular,* 1283, 47.

Ralph, F. M., P. J. Neiman, and G. A. Wick (2004), Satellite and CALJET aircraft observations of atmospheric rivers over the Eastern North Pacific Ocean during the winter of 1997/98. *Mon. Wea. Rev.,* 132, 1721–1745, doi:10.1175/1520-0493(2004)132<1721:SACAOO>2.0.CO;2.

Ralph, F. M., P. J. Neiman, and R. Rotunno (2005), Dropsonde observations in low-level jets over the Northeastern Pacific Ocean from CALJET-1998 and PACJET-2001: mean vertical-profile and atmospheric-river characteristics. *Mon. Wea. Rev.,* 133, 889–910, doi:10.1175/MWR2896.1.

Ralph, F. M., P. J. Neiman, G. Wick, S. Gutman, M. Dettinger, D. Cayan, and A. B. White, (2006), Flooding on California's Russian River—role of atmospheric rivers. *Geophys. Res. Lett.,* 33, (L13801), 5 pp, doi:10.1029/2006GL026689.

Ralph, F. M., P. J. Neiman, G. N. Kiladis, K. Weickmann, and D. W. Reynolds (2011), A multiscale observational case study of a Pacific atmospheric river exhibiting tropical–extratropical connections and a mesoscale frontal wave. *Mon. Wea. Rev.,* 139, 1169–1189, doi:10.1175/2010MWR3596.1.

Ralph, F. M., and M. D. Dettinger (2012), Historical and national perspectives on extreme west coast precipitation associated with atmospheric rivers during December 2010. *Bull. Amer. Meteor. Soc.,* 93, 783–790, doi:10.1175/BAMS-D-11-00188.1.

Ralph, F. M., T. Coleman, P. J. Neiman, R. J. Zamora, and M. D. Dettinger (2013), Observed impacts of duration and seasonality of atmospheric-river landfall on soil moisture and runoff in northern California. *J. Hydrometeor.,* 14, 443–459, doi:10.1175/JHM-D-12-076.1.

Ralph, F. M., and Coauthors (2014), A vision for future observations for western U.S. extreme precipitation and flooding. *Journal of Contemporary Water Resources & Education*, 153, 16–32, doi:10.1111/j.1936-704X.2014.03176.x.

Restrepo, P., D. P. Jorgensen, S. H. Cannon, J. Costa, J. Laber, J. Major, B. Martner, J. Purpura, and K. Werner (2008), Joint NOAA/NWS/USGS Prototype Debris Flow Warning System for Recently Burned Areas in Southern California. *Bull. Amer. Meteor. Soc.,* 89, 1845–1851, doi:10.1175/2008BAMS2416.1.

Rutz, J. J., J. W. Steenburgh, and F. M. Ralph (2013), Climatology characteristics of atmospheric rivers and their inland penetration over the western United States. *Mon. Wea. Rev.,* 142, 905–921, doi:10.1175/MWR-D-13-00168.1.

Saha, S., and Coauthors (2010), The NCEP climate forecast system reanalysis. *Bull. Amer. Meteor. Soc.,* 91, 1015–1057, doi:10.1175/2010BAMS3001.1.

Saha, S., and Coauthors (2014), The NCEP climate forecast system version 2. *Journal of Climate*, 27, 2185–2208, doi:10.1175/JCLI-D-12-00823.1.

Smith, B. L., S. E. Yuter, P. J. Neiman, and D. E. Kingsmill (2010), Water vapor fluxes and orographic precipitation over northern California associated with a landfalling atmospheric river. *Mon. Wea. Rev.,* 138, 74–100, doi:10.1175/2009MWR2939.1.

Stock, J. D., and D. Bellugi (2011), An empirical method to forecast the effect of storm intensity on shallow landslide abundance. *Italian Journal of Engineering Geology and Environment*, Casa Editrice Universita La Sapienza, 1013–1022, doi:10.4408/IJEGE.2011-03.B-110.

Stohl, A., C. Forster, and H. Sodemann (2008), Remote sources of water vapor forming precipitation on the Norwegian West Coast at 60°N—a tale of hurricanes and an atmospheric river. *J. Geophys. Res.*, 113, D05102, doi:10.1029/2007JD009006.

Wieczorek, G. F., and T. Glade (2005), Climatic factors influencing occurrence of debris flows. In *Debris-flow Hazards and Related Phenomena*, edited by M. Jakob and O. Hungr, pp. 325–363. Springer and Praxis Publishing, Berlin, Heidelberg.

Zhu, Y., and R. E. Newell (1998), A Proposed Algorithm for Moisture Fluxes from Atmospheric Rivers. *Mon. Wea. Rev.*, 126, 725–735, doi:10.1175/1520-0493(1998)126<0725:APAFMF>2.0.CO;2.

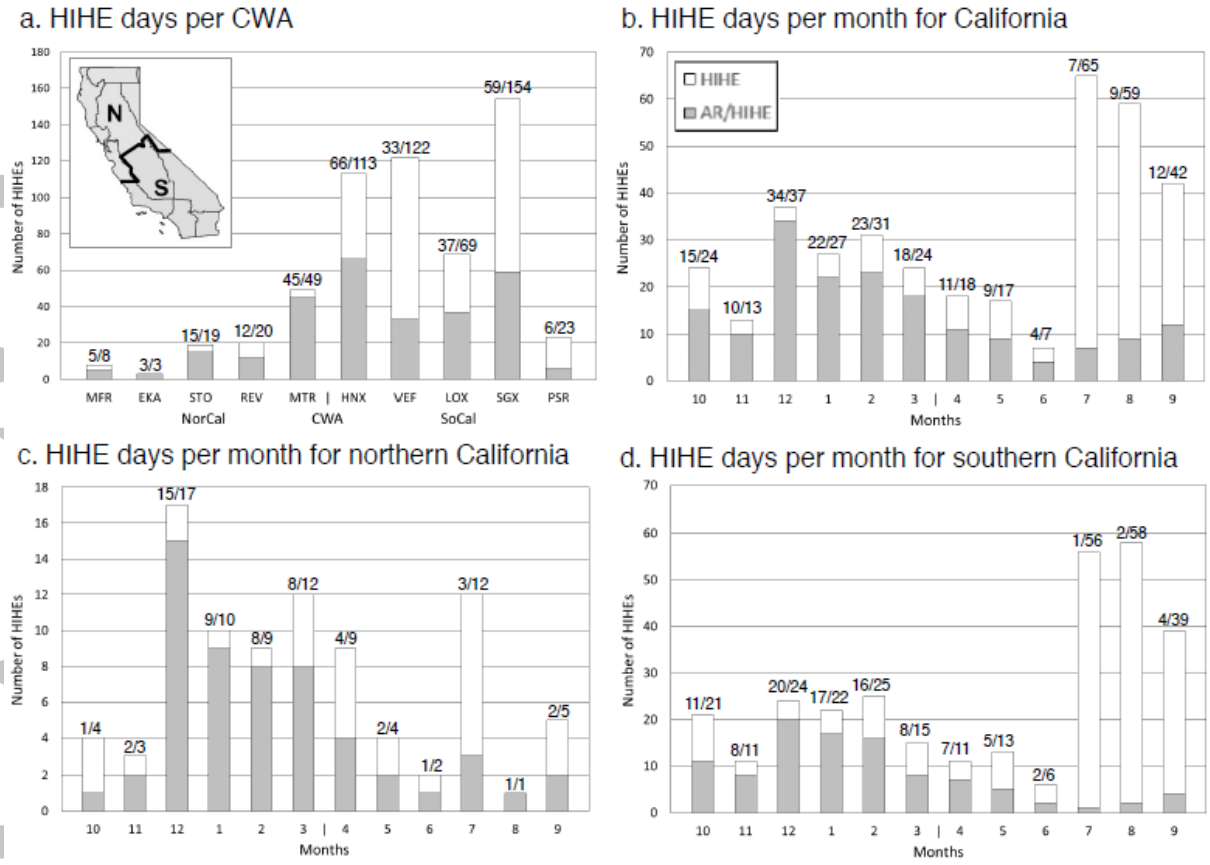


**Figure 1.** Total number of HIHE days per (a) CWA and (b–d) month for (b) all of California, (c) northern California, and (d) southern California. The white bars and denominator represent the total number of HIHE days, whereas the grey bars and numerator represent the total number of HIHE days associated with ARs.

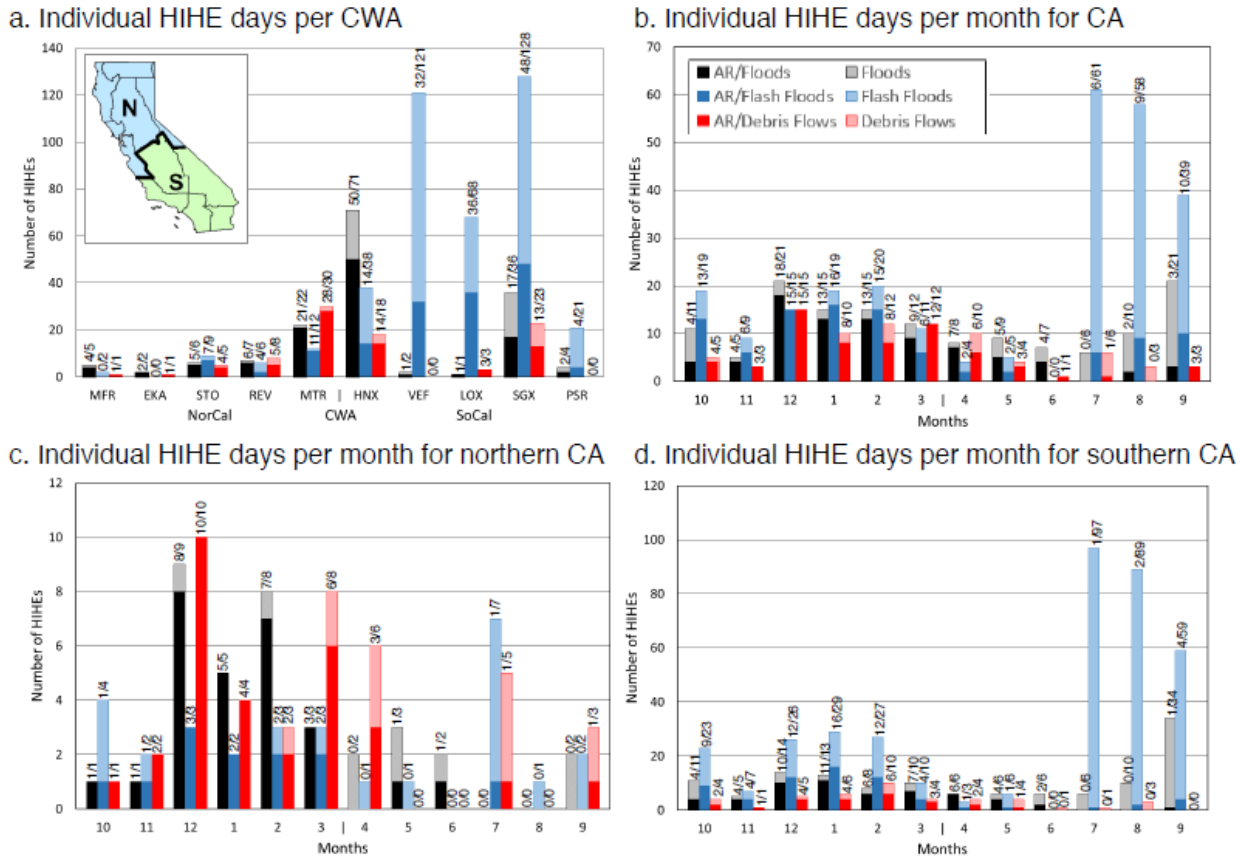


**Figure 2.** As in Fig. 1, except for individual HIHE reports according to the key in panel (b).

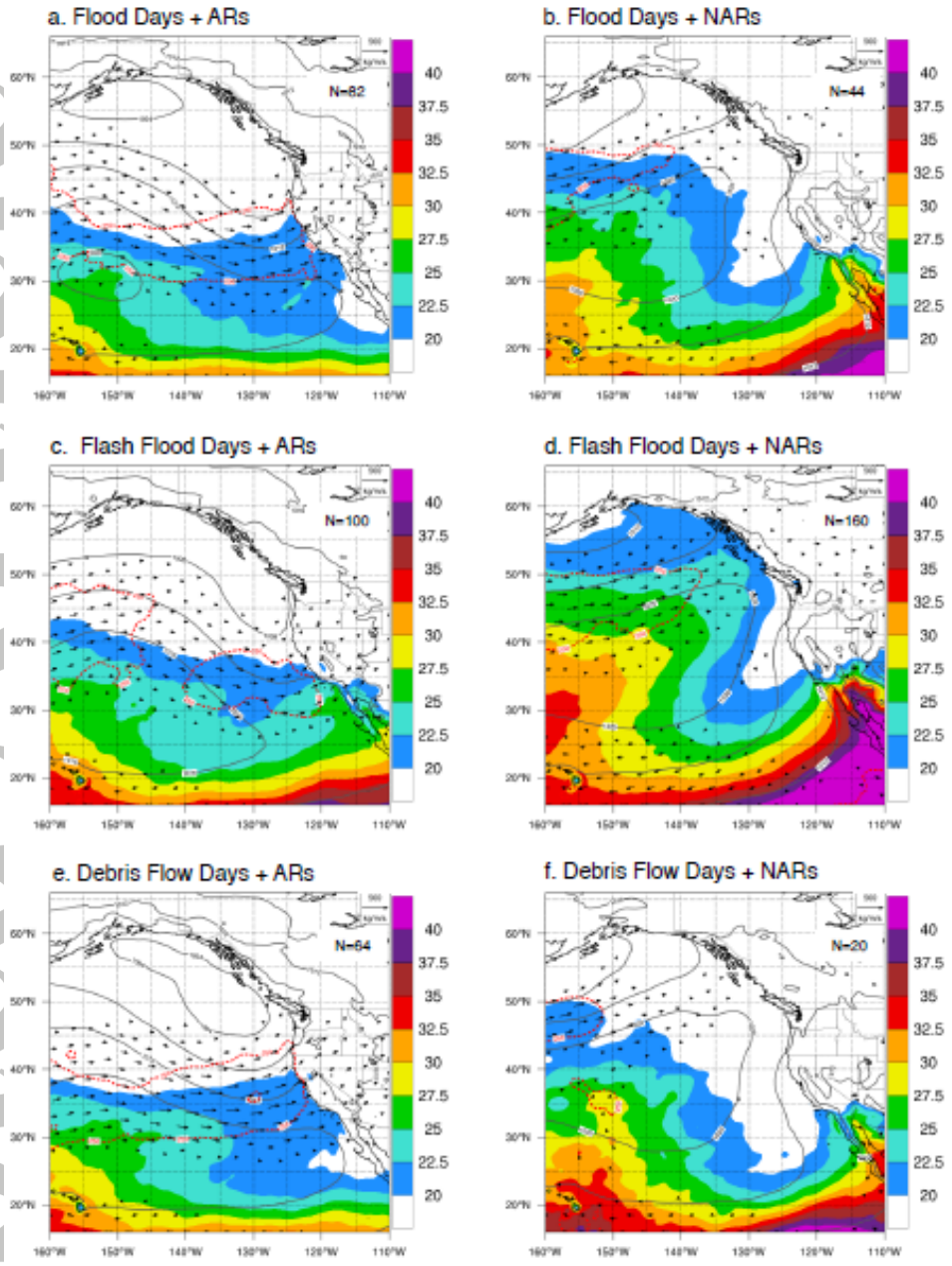


**Figure 3.** Composite analysis sea-level pressure (hPa; contoured), IWV (mm; shaded according to scale), and IVT (kg $m^{-1}$ $s^{-1}$; vectors plotted according to reference and for magnitudes >100 kg $m^{-1}$ $s^{-1}$, and magnitude contoured in red dashed lines every 100 kg $m^{-1}$ $s^{-1}$ beginning at 250 kg $m^{-1}$ $s^{-1}$) on (a) flood days associated with ARs and (b) flood days not associated with ARs across California. (c–f) as in (a) and (b), except for flash flood and debris flow days. The number of composite members is indicated in each panel.

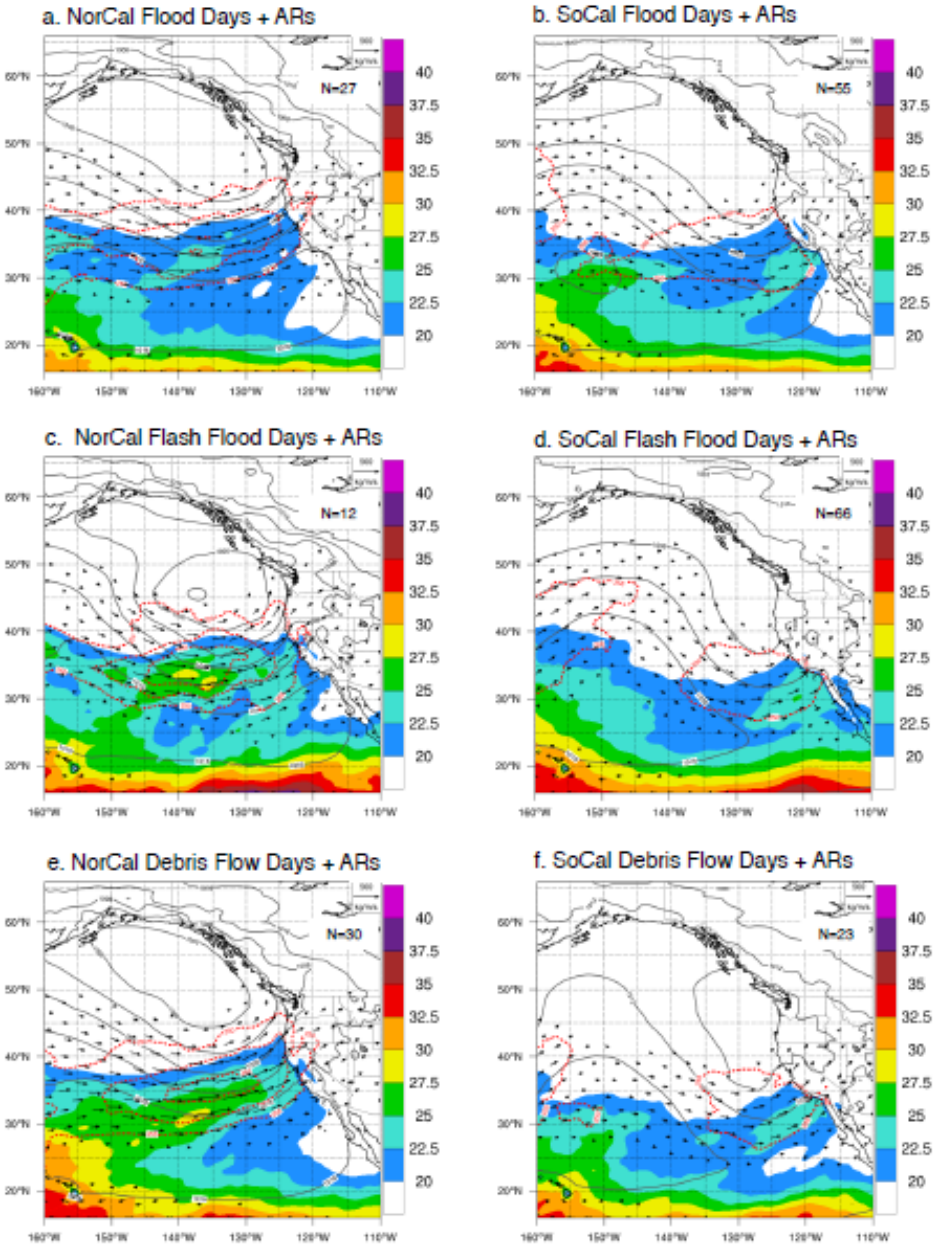


**Figure 4.** As in Fig. 3, except for flood, flash flood, and debris flow days only associated with ARs in (a, c, e) northern California and (b, d, f) southern California.

| Avg Precip Rank | | MFR | EKA | STO | REV | MTR | HNX | VEF | LOX | SGX | PSR |
|---|---|---|---|---|---|---|---|---|---|---|---|
| Floods | AR | 99 | 94 | 96 | 98 | 97 | 95 | 100 | 98 | 97 | 84 |
| | NAR | 92 | - | 54 | 0 | 91 | 73 | 68 | - | 71 | 90 |
| Flash Floods | AR | - | - | 92 | 36 | 99 | 91 | 94 | 96 | 96 | 75 |
| | NAR | 58 | - | 25 | 42 | 58 | 37 | 76 | 71 | 67 | 82 |
| Debris Flows | AR | 97 | 100 | 67 | 98 | 94 | 92 | - | 99 | 96 | - |
| | NAR | - | - | 0 | 58 | 56 | 36 | - | - | 88 | - |

**Figure 5.** Mean areal QPE rank with respect to a 10-WY climatology for CWA 48-h mean areal QPE on the day of and day before HIHE associated with ARs (AR) and not associated with ARs (NAR) by HIHE type: flood days (grey), flash flood days (blue), and debris flow days (pink). The red text denotes that HIHE days associated with ARs contained a higher rank than HIHE days not associated with ARs.